A reassessment of the deep Fiji earthquake of 26 May 1932

Emile A. Okal [*]

Department of Geological Sciences, Northwestern University, Evanston, IL 60201, USA

Abstract

The 1932 deep Fiji earthquake is studied from the point of view of comparing it to the recent large events in the transition zone. Spectral analysis and body-wave modeling suggest a moment of 3.4×10^{27} dyn cm (within a multiplicative or divisive factor of 1.5), which makes it comparable to, but not significantly larger than, the great 1994 earthquake, 770 km to the north. Its seismic moment remains well below that of the largest deep shocks (1994 in Bolivia or 1970 in Colombia). Relocation efforts show that the earthquake took place on the front edge of the Wadati–Benioff Zone, in an area where the latter features a complex geometry involving significant warping. The mechanism of the earthquake involves down-dip compression and can be readily explained in terms of the prevailing large-scale stresses in the slabs.

1. Introduction and background

Large, deep earthquakes are one of our very few windows on dynamic processes in the transition zone. Yet, they occur so rarely as to raise the question whether the few events observed since the implementation of modern instrumental networks (the WWSSN in 1962, followed by the digital networks since 1976) are truly representative of long-term trends in deep seismicity.

In particular, the recent occurrence of three large deep events (Fiji, 09 March 1994; $M_0 = 3.1 \times 10^{27}$ dyn cm; Bolivia, 09 June 1994; $M_0 = 2.6 \times 10^{28}$ dyn cm; Flores Sea, 17 June 1996; $M_0 = 7.9 \times 10^{27}$ dyn cm) has spawned renewed interest in the study of very deep earthquakes. The Bolivian event occurred in an area previously regarded as aseismic; the Flores event was more than 10 times larger than

any other known Indonesian earthquake below 400 km; as for the Fiji earthquake, it shattered the widely perceived concept that large deep shocks do not occur in the Tonga–Fiji region. However, based on frequency–size relationships, Giardini and Lundgren (1995) have argued that the 1994 Fiji earthquake was not unexpected in size, a conclusion also supported by Okal and Kirby's (1995) model for the deep earthquake population of the Fiji–Tonga subduction zone. The argument in both of these studies is that the time window covered by the pre-1994 CMT catalogue (17 years) was simply too short: for the whole Fiji–Tonga–Kermadec subduction zone, and in the depth range 500–600 km, Okal and Kirby's population model would predict one event the size of the 1994 shock only every 64 years.

Indeed, it turns out that a major earthquake occurred around 25°S, 179°E, under the South Fiji Basin, on 26 May 1932. The event was felt in Eastern North Island, New Zealand, at a distance

[*] Fax: +1 (847) 491-8060; E-mail: emile@earth.nwu.edu

of approximately 1900 km (Anonymous, 1932). At the time, this earthquake was given considerable attention, notably by Brunner (1938), who collected a large dataset of original seismograms and wrote a detailed monograph concentrating mostly on the hypocentral location and on the propagation of the various trains of body waves generated by the earthquake. While Brunner mentioned repeatedly its 'extreme violence', the event predated the development of the concept of magnitude, especially for deep shocks (Gutenberg, 1945), and Brunner's comments on its size remain purely qualitative. The magnitude later assigned to the 1932 earthquake by Gutenberg and Richter (1954) is $M = 7\frac{3}{4}$; this is the figure obtained by B. Gutenberg (Seismological Society of America, 1980), although the computerized NEIC database reports a Pasadena magnitude $M_{PAS} = 7.9$. The origin of this discrepancy is unclear. At any rate, this is the highest magnitude found in Gutenberg and Richter (1954) for a post-1920 transition zone earthquake. (The Fiji earthquake of 16 April 1937 is also given $M = 7\frac{3}{4}$, but the depth of this event is poorly constrained, and its moment is probably not greater than 10^{27} dyn cm; Okal, 1992b.) Similarly, Abe and Kanamori (1979) assign a 6-s body-wave magnitude $m_B = 7.5$ to both the 1932 and 1937 shocks, a figure surpassed only by a 1909 Fiji event ($m_B = 7.6$) in the general vicinity of the 1994 earthquake.

In this context, the reassessment of the exact location, size and possible mechanism of the 1932 earthquake is an important issue in the general context of the dynamics of the transition zone. Given the abundance of superlatives in Brunner's (1938) description of the body phases of the event, we seek a quantitative answer to the simple question of its moment: was the 1932 shock as large as the 1994 Fiji earthquake? or could it have been even larger and comparable to the 1994 Bolivian or 1970 Colombian events?

2. Relocation

The purpose of this section is to use published arrival times to precisely relocate the hypocenter of the 1932 Fiji earthquake, following the iterative interactive algorithm described in detail in Wysession et al. (1991). However, before we can proceed with a relocation effort, the first challenge is to address the complex character of the 1932 event. The April–June 1932 issue of the International Seismological Summary (1937; hereafter 'the ISS') lists two shocks, at 16 : 09 : 19 GMT and 16 : 09 : 29, respectively, both at 24.0°S, 179.2°E, and at a depth $h = 350$ km. Gutenberg and Richter (1954) list a single event, at 16 : 09 :40, $25\frac{1}{2}$°S; $179\frac{1}{4}$°E, $h = 600$ km. Through his close inspection of seismograms, Brunner (1938) suggests that there were actually three events, a weak first shock, followed 3 or 4 s later by a stronger event clearly seen at all stations, and then 12 s later by the main energy release, which he places at 25°S, 179.4°E, $h = 600$ km, with an origin time of 16 : 09 : 58 GMT. The difference in depth between the ISS solution and Brunner's can account for a lag of about 23 s in origin time, which in turn suggests that the main (second) ISS event represents a combination of Brunner's second and third shocks. This idea is supported by the large scatter in ISS residuals, which, because they do not correlate with distance, cannot be an artifact of erroneous depth alone.

2.1. Association of arrival times

We first attempted to relocate the second ISS entry (pp. 169–171) as a single event; the best r.m.s. residual obtained is $\sigma = 4.8$ s at a depth of 195 km, which is irreconcilable with the dataset of reflected phases (see below); if the depth is constrained at 560 km, σ remains high (5.19 s), with the residual population strongly bimodal around values of ±5 s. Thus, we proceeded to split the arrival time population into two groups on the basis of this observation, assuming that the groups relate to two separate shocks, which we call the second and third events. Similarly, in the case of the foreshock (1st ISS entry, pp. 168–69), we reassigned to the second event the arrival at Takaka, New Zealand, which features an excessively positive residual (6.6 s).

Note that because we have split arrival times originally reported as P waves of the same assumed source, the datasets for the second and third events share no station, and thus it is not possible to use the classic methods of Joint Hypocenter Determination (Douglas, 1967) or Centroid Relocation (Sverdrup and Jordan, 1981) to relocate the events relative to each other. Finally, because of the strong thermal ef-

fects known to take place in the hypocentral regions, we made no use of S times, which would be expected to show particularly large anomalies.

2.2. Relocation

The foreshock converges to a depth of 549 km with $\sigma = 2.55$ s, a figure much more in line with the expected quality of relocations for that era, based on our previous experience (Wysession et al., 1991). Similarly, the second event converges to 483 km ($\sigma = 1.33$ s), and the third one to 523 km ($\sigma = 2.38$ s). However, the datasets of P arrival times clearly have no depth resolution, as documented by a series of Monte Carlo statistical tests consisting of performing 400 relocations of each event after injection of random noise into the dataset (Wysession et al., 1991). The resulting hypocentral depths range from 253 km to 756 km, from 291 to 764 km, and from 208 to 760 km, respectively, for the three shocks, and this with a standard deviation of the Gaussian noise of only 3 s, a somewhat conservative value for an earthquake in the 1930s. Thus it becomes necessary to independently constrain the source depths in order to stabilize the relocations.

As explained by Brunner (1938), the only later phases which can be unambiguously associated with one of the sources are those relating to the third event, which involves the largest energy release. Based on his extensive dataset, we find an average (pP–P) time of 122.5 s around $\Delta = 100°$, corresponding to a depth of 555 km using the iaspei91 tables (Kennett and Engdahl, 1991). Similarly, (sS–S) times suggest 560 km, and (sP–P), 570 km. Accordingly, we elected to constrain the depth of the third (main) event at 560 km, which is significantly shallower than the 600 km suggested by both Brunner (1938) and Gutenberg and Richter (1954). It is worth noting that Brunner's original calculation yields a depth of 570 km, and his application of the method by Stechschulte (1932) led him to 573 km. Later in his paper, Brunner revises the figure to 600 km, accounting for what we would call nowadays lateral heterogeneity. In so doing, he uses evidence obtained in Japan of fast velocities for rays propagating directly from a deep focus to a nearby station, most probably up the slab. However, Brunner then assumes that this fast velocity could be applied to all teleseismic pP phases radiated from the earthquake, when we now know that the back-arc basin will actually feature slower-than-average velocities. Thus, we do not think that Brunner's final correction is sound, and believe that his dataset actually calls for a depth of 560 ± 10 km. Based on the lack of depth resolution in the P datasets for the first and second events, we also elected to constrain their depths at 560 km.

Constrained-depth relocations then converge on the parameters listed in Table 1. Note that the quality of the locations, as given by the r.m.s. residuals σ, are not significantly degraded with respect to floating depth solutions. The time lags obtained between the various sources (5.3 s and 8.8 s) are in reasonable agreement with the numbers proposed by Brunner (3 or 4 s, then 12 s). Our earlier origin times simply reflect the shallower depths. The relocated epicenter for the main shock is significantly west of all other locations (ISS, Brunner, Gutenberg and Richter; see Fig. 1).

The relative distances between the various components of the source are 92 km (Event 1 to Event 2), and 56 km (Event 2 to Event 3). If interpreted in terms of the simple propagation of rupture from one event to the next, these would suggest very high or even unrealistic rupture velocities (17 and 6 km/s, respectively). However, the shape of the ellipse errors would reduce these numbers considerably, to a value close to the ambient S-wave velocity, if one assumes that the location of Events 1 and 2 are close to the northwestern and eastern extremities of their confidence ellipses, respectively.

2.3. Aftershocks

The ISS lists three aftershocks following the main shock by 6, 9 and 13 h, respectively. In the case of the first one (A-1 in Table 1), the dataset has once again poor depth resolution, with the Monte Carlo hypocenters ranging from 425 to 643 km. When constrained to 560 km, the source moves to a location approximately 83 km southeast of the main shock. It is worth noticing that the ISS locations feature a similar displacement of the epicenter. The second aftershock locates about 58 km south of the main shock. As for the third aftershock, it was recorded only in Samoa, New Zealand and California, and its location

Table 1
Relocation results

Event Nr.	Date	Lat. (°N)	Long. (°E)	Depth (km)[a]	Origin time (GMT)	Number of stations	σ (s)	Bulletin magnitude[b]
Main shock sub-events								
1	26 May, 1932	−25.12	178.70	560	16:09:37.6	30	2.55	
2	26 May, 1932	−24.77	177.77	560	16:09:42.9	25	1.36	
3	26 May, 1932	−24.97	178.34	560	16:09:51.7	27	2.39	$7\frac{3}{4}$ G–R
Aftershocks								
A-1	26 May, 1932	−25.45	179.12	560	22:21:51.4	20	1.80	$6\frac{1}{2}$ G–R
A-2	27 May, 1932	−25.54	178.46	560	01:29:45.0	12	1.11	$6\frac{1}{4}$ G–R
A-3	27 May, 1932	−24.87	−178.89	500	05:55:20.0	8	1.54	$5\frac{3}{4}$ G–R
Neighboring large historical earthquakes								
	18 October, 1931	−26.00	−179.99	455 F	04:30:33.5	28	2.52	$6\frac{3}{4}$ G–R
	10 October, 1934	−23.34	179.60	500 F	15:42:07.6	55	1.88	7.3 G–R
	15 December, 1934	−23.34	−179.92	495 F	19:14:28.4	39	1.84	6.9 G–R
	01 August, 1940	−25.93	179.64	434 F	12:39:32.1	30	2.44	$6\frac{3}{4}$ G–R
	29 August, 1942	−23.91	178.98	529 F	01:39:21.7	14	1.59	$6\frac{3}{4}$ G–R
	26 September, 1946	−25.34	178.18	537 C	10:53:10.3	27	1.98	7.0 G–R
	08 October, 1946	−24.98	178.09	581 F	13:56:19.9	20	1.83	$6\frac{3}{4}$ G–R
	08 September, 1951	−24.78	−179.69	446 F	16:15:21.8	21	0.80	$6\frac{3}{4}$ WEL

[a] C = constrained; F = floated.
[b] G–R Gutenberg and Richter (1954); WEL: Wellington Observatory.

is very poorly constrained in the ESE–WNW direction: Monte Carlo relocations could place it about 100 km northeast of the main shock, but the most probable location would be around 25°S, 179°W, in a zone of documented, albeit sparse, seismicity at a depth of 500 km (29 February 1984, $m_B = 5.0$; 10 October 1988, $m_B = 4.9$), in which case it could be unrelated to the occurrence of the main shock. Fig. 1 presents the general layout of the Monte Carlo ellipses for the various sources.

In addition to these events, recorded at large tele-seismic distances, the Wellington Dominion Observatory (WEL) lists four more shocks, following the main shock by 7, 26, 135, and 177 min, respectively (Anonymous, 1932). These reports are from station WEL exclusively. The first of those has an excessive S–P (200 s as opposed to the expected 167 s from the main hypocenter), and is labeled 'confused with previous shocks'; these readings may not represent a genuine aftershock, but rather a combination of later phases from the main shock. The other three aftershocks are given S–P times in generally good agreement with the expected hypocenter (164, 170, and 149 s, respectively). Thus, out of the seven after-shocks previously mentioned for this event (Guten-

berg and Richter, 1938; Wiens and McGuire, 1995), we regard five as confirmed (A-1, A-2, and the last three reported by Wellington), while the other two are doubtful. As noted by Wiens and McGuire (1995) and Wiens et al. (1995), the identification of aftershocks under the poor detection thresholds of the 1930s supports the general observation that deep Fiji earthquakes generate larger aftershock populations than events from other subduction zones.

3. Seismic moment

The purpose of this and the next sections is to obtain an estimate of the moment of the earthquake. In particular, we wish to compare it to events such as the 1994 Fiji earthquake (3×10^{27} dyn cm) or the gigantic 1970 Colombia and 1994 Bolivia shocks ($2 - 3 \times 10^{28}$ dyn cm). With this goal in mind, we attempted to gather a suitable set of records on instruments with well-documented responses. As discussed in Okal (1992b), such an endeavor requires firm knowledge of instrument calibrations, and unfortunately, this reduces substantially the number of usable records. The location of the event adds to the difficulty, since most regions well instrumented at
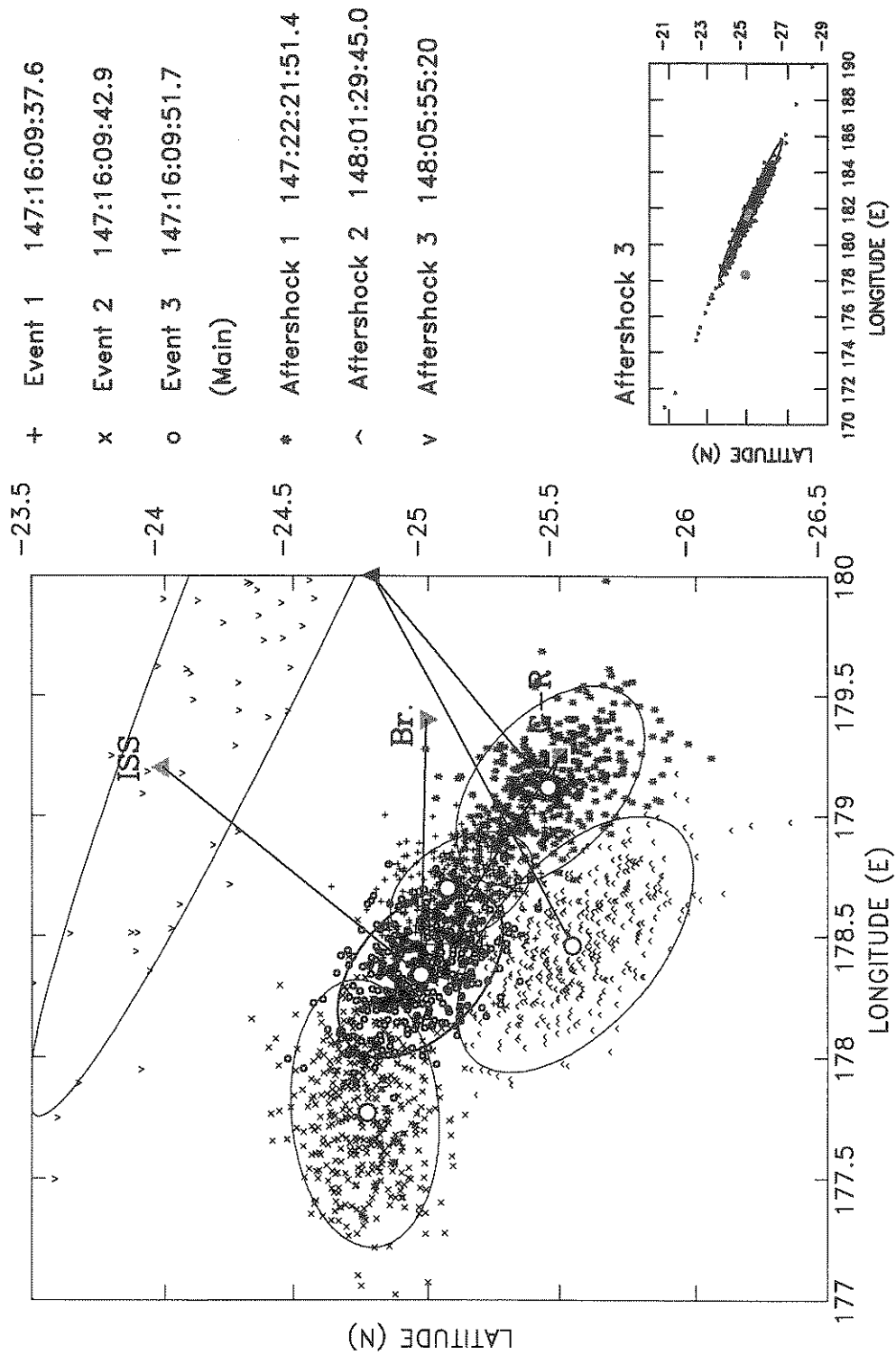
Fig. 1. Relocation of the subevents and aftershocks of the 1932 deep Fiji earthquake (see Table 1 and text for details). The circles are the preferred epicenters, surrounded by the relevant Monte Carlo solutions (showed with various symbols), and their best-fitting ellipses. Straight lines link the preferred epicenters to solutions published by the ISS (upward-pointing triangles), Gutenberg and Richter (1954) (squares) and Brunner (1938) (downward-pointing triangle). In the case of Aftershock 3, the smaller map at the right shows that the solution is very poorly constrained (the gray dot at the left of the cluster is the mainshock).

Table 2
Records used

Station	Code	Distance (°)	Azimuth (°)	Instrument	Components	Nature of record [a]	Orientation information	Response information
Tokyo, Japan	TOK	70.64	327.36	Wiechert	Z	C	Yes	Yes
Berkeley, California	BRK	83.87	43.35	Wiechert	Z	O	No	Yes
Berkeley, California	BRK	83.87	43.35	Bosch-Omori	EW	O	Yes	Yes
Pasadena, California	PAS	84.28	48.34	Wood-Anderson	NS, EW	O	Yes	Yes
Saint Louis, Missouri	SLM	106.25	54.77	Wood-Anderson	NS, EW	O	No	No
Sverdlovsk, Russia	SVE	125.69	323.00	Galitzin	Z, NS, EW	O	Yes	Yes
Pulkovo, Russia	PUL	138.75	335.86	Galitzin	Z, NS, EW	O	Yes	Yes
Uppsala, Sweden	UPP	142.64	343.95	Wiechert	NS, EW	S	Yes	Yes
Stuttgart, Germany	STU	154.72	342.69	Wiechert	Z	C	No	Yes

[a] C = copied from Brunner (1938); O = copy of original seismogram; S = photographic slide of original seismogram.

the time (North America, Europe) are in or beyond the core shadow; also, the event predates by a few years the development of both the strainmeter and 1-90 Benioff instruments at Pasadena.

Through a systematic search of various historical seismogram collections, and visits to several observatories, we were able to gather the records listed in Table 2. In addition, a remarkable set of seismograms from the event is reproduced in Brunner (1938), although in many instances, it was difficult to retrieve precise focal constraints from these records, the complexity of the source making it difficult to unambiguously pick the first arrival, and information on orientation and response (McComb and West, 1931) being often inadequate. In addition, many of the records copied by Brunner are windowed around seismic phases more remarkable for their general amplitude than for their potential for resolving the focal geometry.

3.1. Direct estimate of the moment

We first attempted to obtain an estimate of the size of the 1932 earthquake relative to the more recent, well-measured events, irrespective of its focal mechanism. For this purpose, we sought to use a mantle magnitude measurement (Okal, 1990). Unfortunately, we observed that mantle Rayleigh and Love waves were recorded above noise level neither on the narrow-band electromagnetic instruments (Galitzin-type), with typical maximum magnification of 1000 and sensitive in a frequency band weakly excited by deep earthquakes, nor on the mechanical (Wiechert-

type) instruments, relatively more sensitive to mantle waves, but suffering from generally lower absolute magnifications (typically 200). Thus, no mantle magnitude M_m could be computed. This in turn suggests that the moment of the 1932 earthquake must remain below 10^{28} dyn cm (Okal, 1992b).

Similarly, we could not use the overtone Rayleigh wave train ${}_1R$. While this phase is well excited by deep earthquakes (Okal, 1979), and was prominent in the 10–15 mHz range on records of the Colombian and Bolivian events, it is expressed mostly on the vertical component (Okal and Jo, 1983); the very few vertical instruments operating at the time were usually higher frequency than the horizontal ones, with the result that the first overtone is not displayed above noise level. In practice, no surface waves can be used to assess the moment of the earthquake.

3.2. Spectra

Another approach to the investigation of the moment of the earthquake independently of its focal mechanism is to study the spectrum of ground motion for long time windows, and to compare it to events of known moment recorded at similar distances. By using very long windows on both horizontal components, we hope to include many seismic phases, and thus to compensate to some extent for any expected difference in exact depth and focal mechanism. We emphasize that this exercise aims at providing more of an order of magnitude than a precise value of the seismic moment.
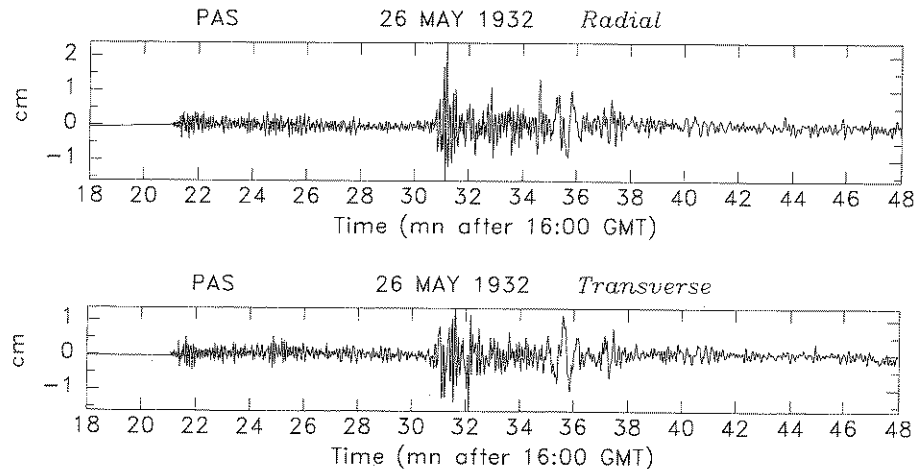
Fig. 2. Pasadena torsion seismograms of the 1932 deep Fiji earthquake, after digitization and rotation into natural polarization.

We selected for analysis the 1932 Pasadena records (Fig. 2), which are written on well-documented torsion seismometers ($T = 6$ s; $V = 800$; $\varepsilon = 0.8$). We chose to compare them with those for four recent deep earthquakes, listed in Table 3, and whose moments span two orders of magnitude. For each event, we attempted to find a station at a similar distance, and produced spectra of hour-long horizontal seismograms after rotation into radial (R) and transverse (T) components. We also plot on these figures the threshold of noise on the 1932 records, estimated in the manner of Okal (1992a). However, in this particular case, we define it as $n(t) = 0.5$ mm, on account of the generally coarser nature of seismogram traces on photographic paper, as compared to the mechanical smoke-paper records of the Wiechert instrument considered in Okal (1992a).

The following observations are readily made from Fig. 3.

(1) The four recent earthquakes are well separated at low frequencies, and their two components (radial and transverse) have generally comparable spectral levels. This justifies the concept of using them as moment benchmarks.
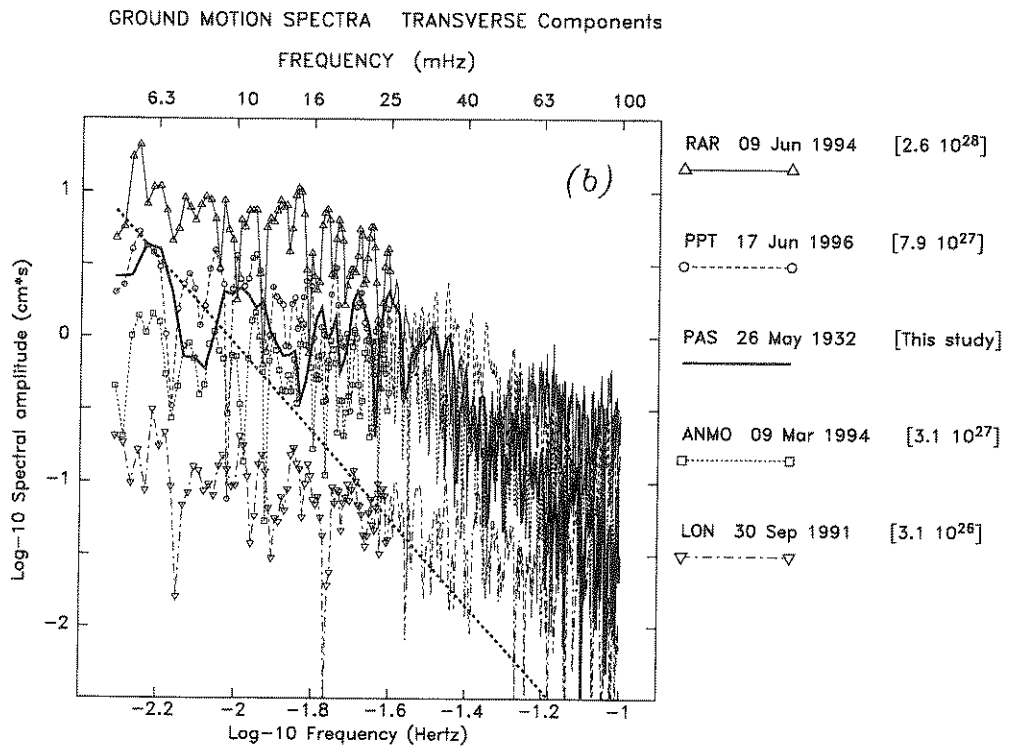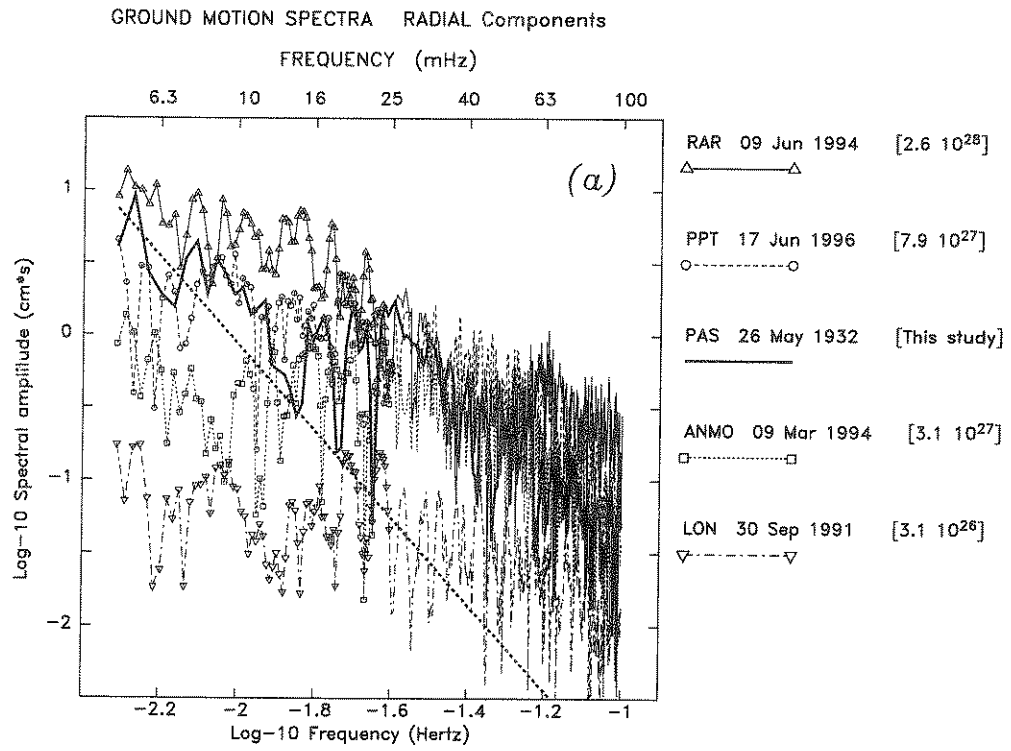
(2) The 1932 earthquake is significantly larger than the smaller 1991 Fiji event at all frequencies considered.

(3) In the 40 mHz frequency range, the spectral levels of all four remaining earthquakes are very similar.

(4) Between 12 and 25 mHz, the spectra of the two Fiji earthquakes (1932 and 1994) taper off at values of 1 cm*s (1932; T and R), 0.8 cm*s (1994; T) and 0.7 cm*s (1994; R), while that of the Indone-

Table 3
Earthquakes and records used in the spectral analysis (Fig. 3)

Earthquake						Station	
region	date	epicenter		depth (km)	moment (10^{27} dyn cm)	code	distance (°)
		°N	°E				
This study							
Fiji–Kermadec	26 May, 1932	−25.0	178.3	560		PAS	84.28
Benchmark							
Bolivia	09 June, 1994	−13.8	−67.6	638	28	RAR	87.07
Flores Sea	17 June, 1996	−7.1	122.6	589	7.9	PPT	85.81
Fiji	09 March, 1994	−18.0	−178.4	568	3.1	ANMO	86.22
Fiji	30 September, 1991	−20.7	−178.5	590	0.31	LON	84.45

E.A. Okal / Tectonophysics 275 (1997) 313–329

GROUND MOTION SPECTRA   RADIAL Components

(a)

GROUND MOTION SPECTRA   TRANSVERSE Components

(b)

sian earthquake reaches 2 cm*s, and the spectrum for Bolivia keeps increasing to about 7 cm*s. Below 12 mHz, the 1932 spectra are marginally, if at all, above noise level, and no comparison can be attempted.

The conclusion from this exercise is that the 1932 earthquake can be best described as intermediate in size between the 1994 Fiji and 1996 Flores events. It remains, however, much smaller than the 1994 Bolivian earthquake. Further quantification is difficult, because of the many factors (focal mechanism, nature of the body phases, differences in depth) overlooked in this procedure. However, we believe that these comparisons constrain the moment of the 1932 shock to a range of 3–6×10^{27} dyn cm.

4. Focal mechanism

4.1. Attempt at CMT inversion

Because of the complexity of the source, it remained impossible to invert directly for the moment tensor of the source, using the single-station algorithm developed by Huang et al. (1994). Low-pass filtering, a technique successfully used to process complex modern events (Russakoff et al., 1996) could not alleviate this problem, due to the poor response of the historical instruments at the lower frequencies (see Fig. 3). Finally, multi-station inversions proved generally impossible, most probably because of uncertainties on relative timing at the various stations.

Under the assumption of a double-couple mechanism, a number of significant constraints can be put on the geometry of the earthquake, on the basis of the polarity of P, SH, SV and SKS phases, their associated surface reflections, and amplitude ratios such as SH/SV, sS/S, etc., following the general methods of Okal (1984) and Stein et al. (1987). The class of solutions compatible with these constraints require down-dip compression, and can be described as mostly normal faulting on a plane dipping steeply in a northeasterly direction.

4.2. Forward modeling

The fine tuning of the mechanism ($\phi = 330°$; $\delta = 68°$; $\lambda = 310°$ in the notation of Kanamori and Cipar (1974); Fig. 4) was obtained from body-wave forward modeling. Because of source complexity, this procedure was restricted to the following two records written on long-period instruments (with eigenperiods of at least 10 s).

4.2.1. Tokyo, vertical

This record is taken from Brunner (1938). The polarity of the record is documented on the seismogram itself, and the very clear time marks constrain the photographic amplification. The record is labeled (in an overprint by Brunner) as a vertical Omori seismogram. However, McComb and West (1931) do not document such a long-period instrument at Tokyo station. The only documented vertical instrument with characteristics (period, paper speed, etc.) in agreement with the published record is the long-period Wiechert system, and we believe that the seismogram was actually written on that instrument. The generalized P wave (P, pP, sP) was modeled using the ray synthetic seismogram algorithm described by Stein and Wiens (1986), adapted (notably through an Earth-flattening transformation) to handle deep sources. A comparison of observed and synthetic seismograms is given in Fig. 5. The moment required to match the amplitudes is 3.6 × 10^{27} dyn cm.

4.2.2. Stuttgart, vertical

This remarkable record is taken from Brunner (1938). We believe, however, that it was printed upside down (presumably to restore the traditional increase of time to the right), since the strong impulsive PKP_{df} (P'_1 on the record) should be of the same polarity (dilatational) at the nearby European station UPP, where the instrument orientation was controlled in situ by the author at the Uppsala Observatory, and whose ray leaves the source only 3°

Fig. 3. (a) Pasadena spectra of the radial component of ground motion for the deep 1932 Fiji event (thick trace) compared with other large events of known moments (right, in dyn cm), recorded at a similar distance (see Table 3 for details). The thick dashed line is an estimate of the noise level of the torsion instrument at Pasadena. In the range 12–25 mHz, these results suggest that the 1932 earthquake is intermediate in size between the 1994 Fiji and 1996 Indonesia events. (b) Same as (a) for the transverse component.
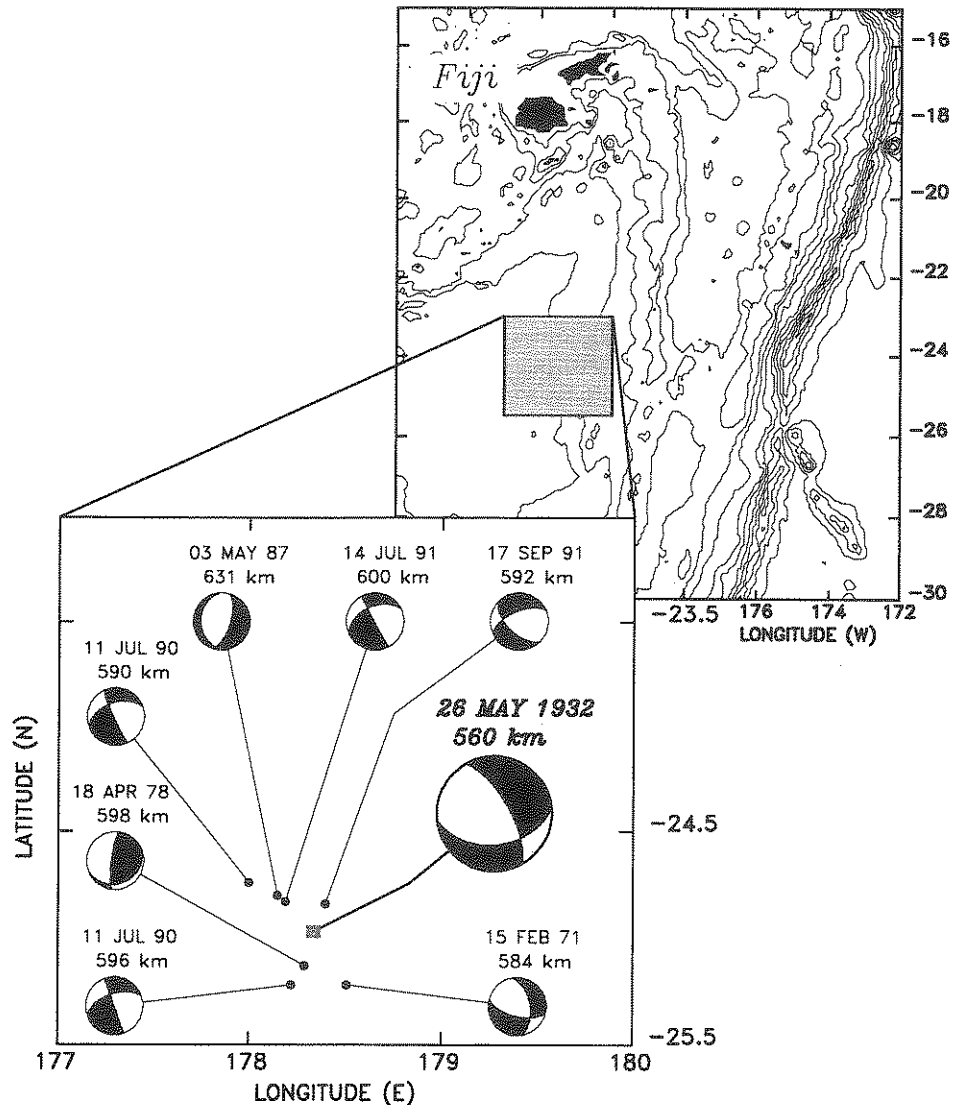
Fig. 4. Focal mechanism of the 1932 earthquake, as determined in this study. We also show CMT solutions in the immediate vicinity of the event, as available from Dziewonski et al. (1983, and subsequent quarterly updates) and Huang et al. (1997). Their spatial distribution is shown in map view. The background map at the upper right sets the study area (shaded) into the familiar bathymetry of the Fiji–Tonga–Kermadec region. The separation of isobaths is 1000 m.

away from that to STU. The primary phases at this distance (154.7°) are the various PKP branches and their associated depth phases, as well as SKP and PKS.

The record was modeled by a reflectivity code (T.J. Clarke, pers. commun., 1995). The final fit is obtained for a source with two pulses separated by 8 s, the total moment required being 2.5×10^{27}

dyn cm. A comparison of data and synthetic is given on Fig. 6. An excellent fit is obtained, except for the frequency content of sSKP, which is of generally lower frequency in the data. This is probably due to propagation through the actively spreading Fiji back-arc basin.

In conclusion, the source of the 1932 earthquake can be best modeled by a double couple having the
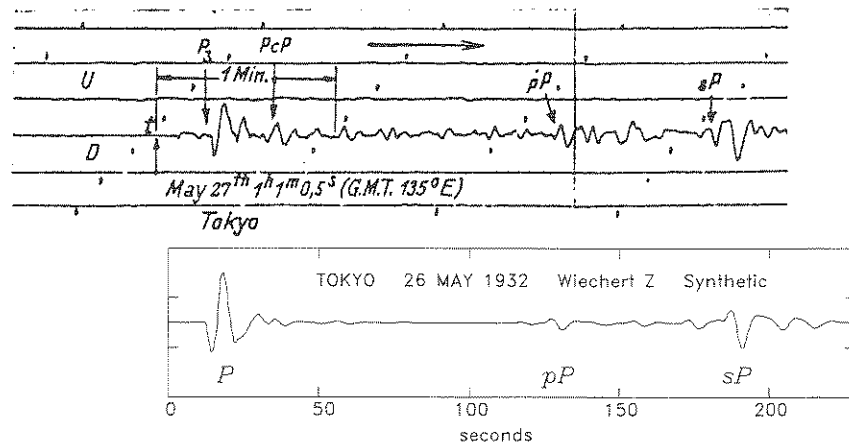
Fig. 5. Observed (top) and synthetic (bottom) seismograms for the vertical instrument at Tokyo ($\Delta = 70.64\ddot{e}$). The observed seismogram is reproduced from Brunner (1938). The vertical scale on the synthetic is arbitrary; as mentioned in the text, the moment needed to match the amplitudes is 3.6×10^{27} dyn cm.

geometry of Fig. 4 with a moment of 3.4×10^{27} dyn cm, this number representing the geometrical average of the three estimates given above. It is difficult to provide formal error bars, but we found that the angles of the focal mechanism cannot be

rotated more than 10° before significant distortion occurs in the relative size of the various phases, notably in the STU record. The scatter of moment values obtained above suggests that the moment proposed is probably accurate within a factor of 1.5,
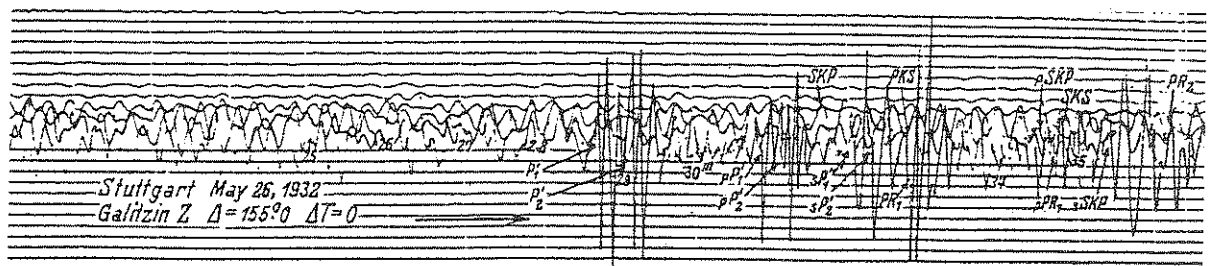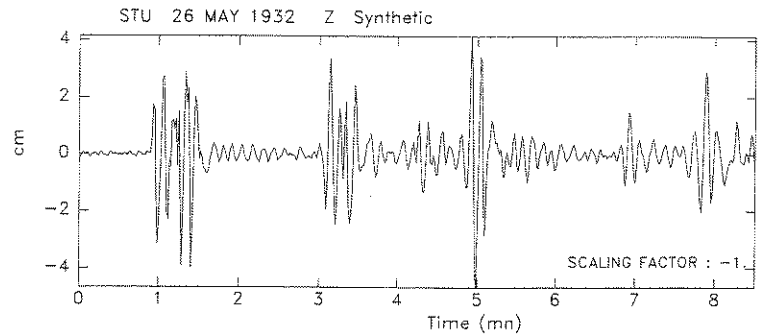

Fig. 6. Observed (bottom) and synthetic (top) seismograms for the vertical Galitzin instrument at Stuttgart ($\Delta = 154.72\ddot{e}$). The observed seismogram is reproduced from Brunner (1938). Phases indexed 1 and 2 refer to Brunner's first and second sub-events, which correspond to our Events 2 and 3 in Table 1. The polarity of the synthetic has been reversed to facilitate comparison (see text for details).
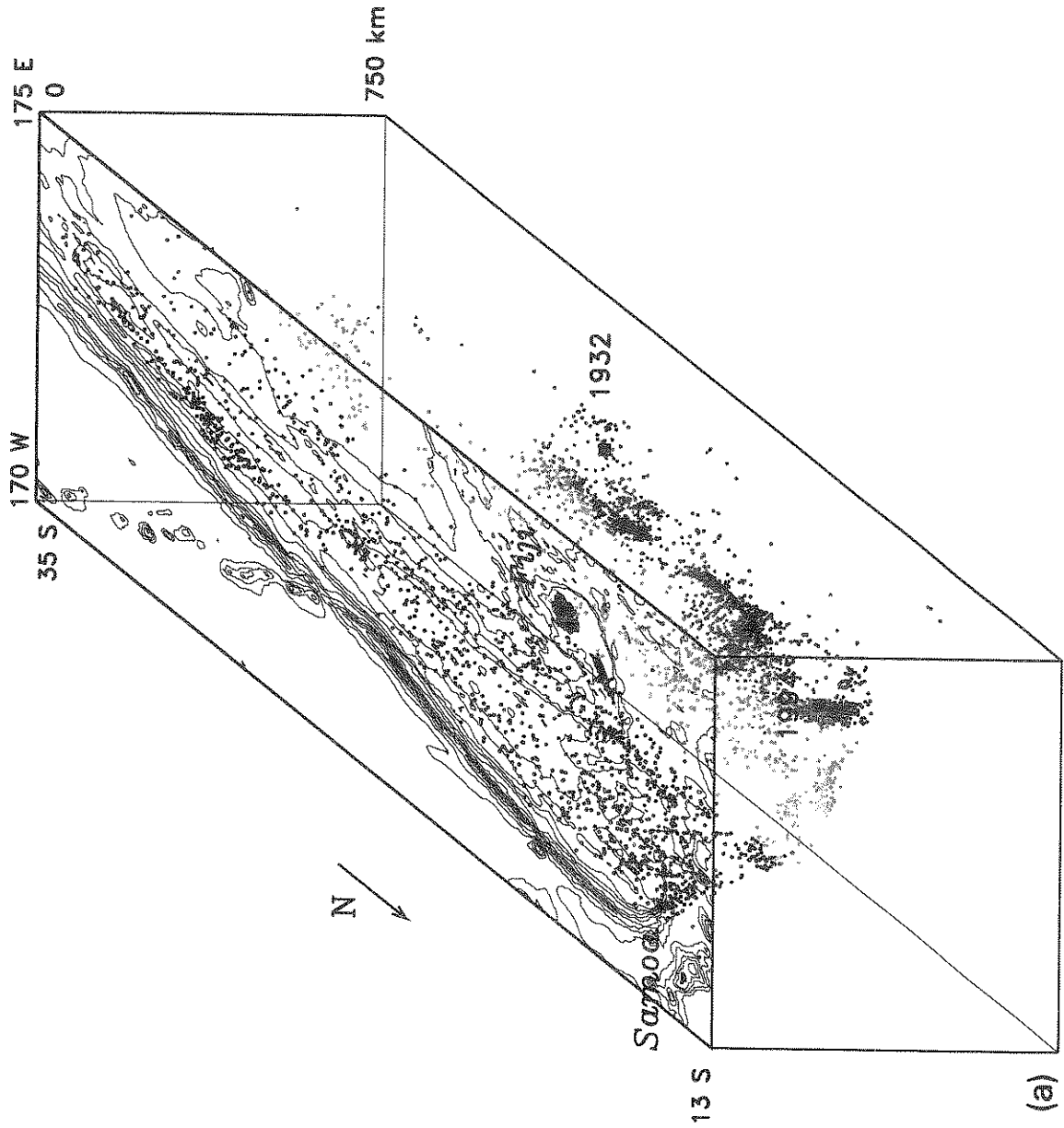
Fig. 7. (a) Three-dimensional view looking southeast of the location of the 1932 event in relation to the Fiji–Tonga–Kermadec Wadati–Benioff zone. The bathymetry is contoured at 1000 m intervals. The seismicity is plotted from the catalogue by Engdahl et al. (1997). Note that the 1932 event takes place near a local boundary of the active zone, in an area of the WBZ exhibiting a complex, warped, shape.
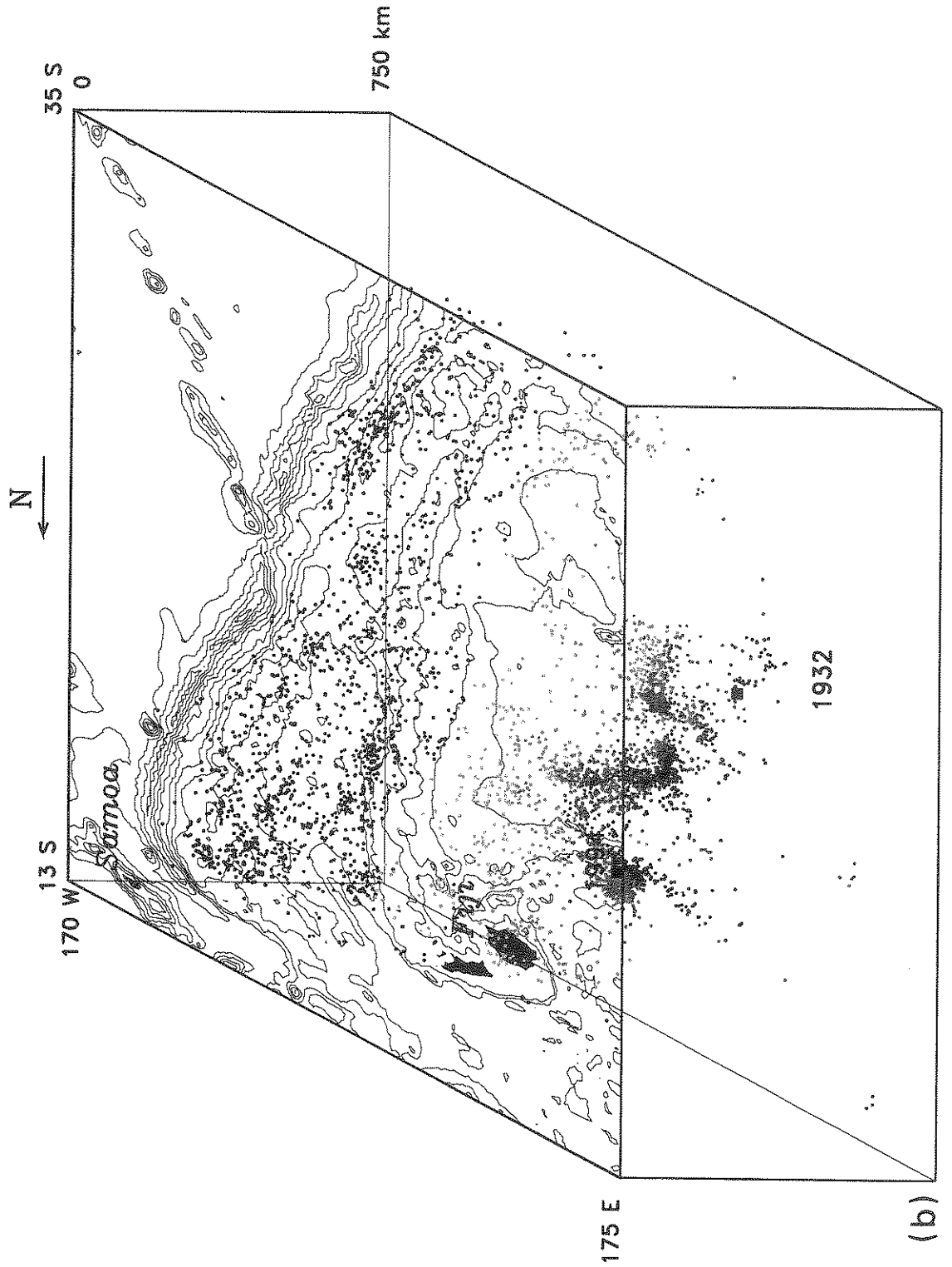
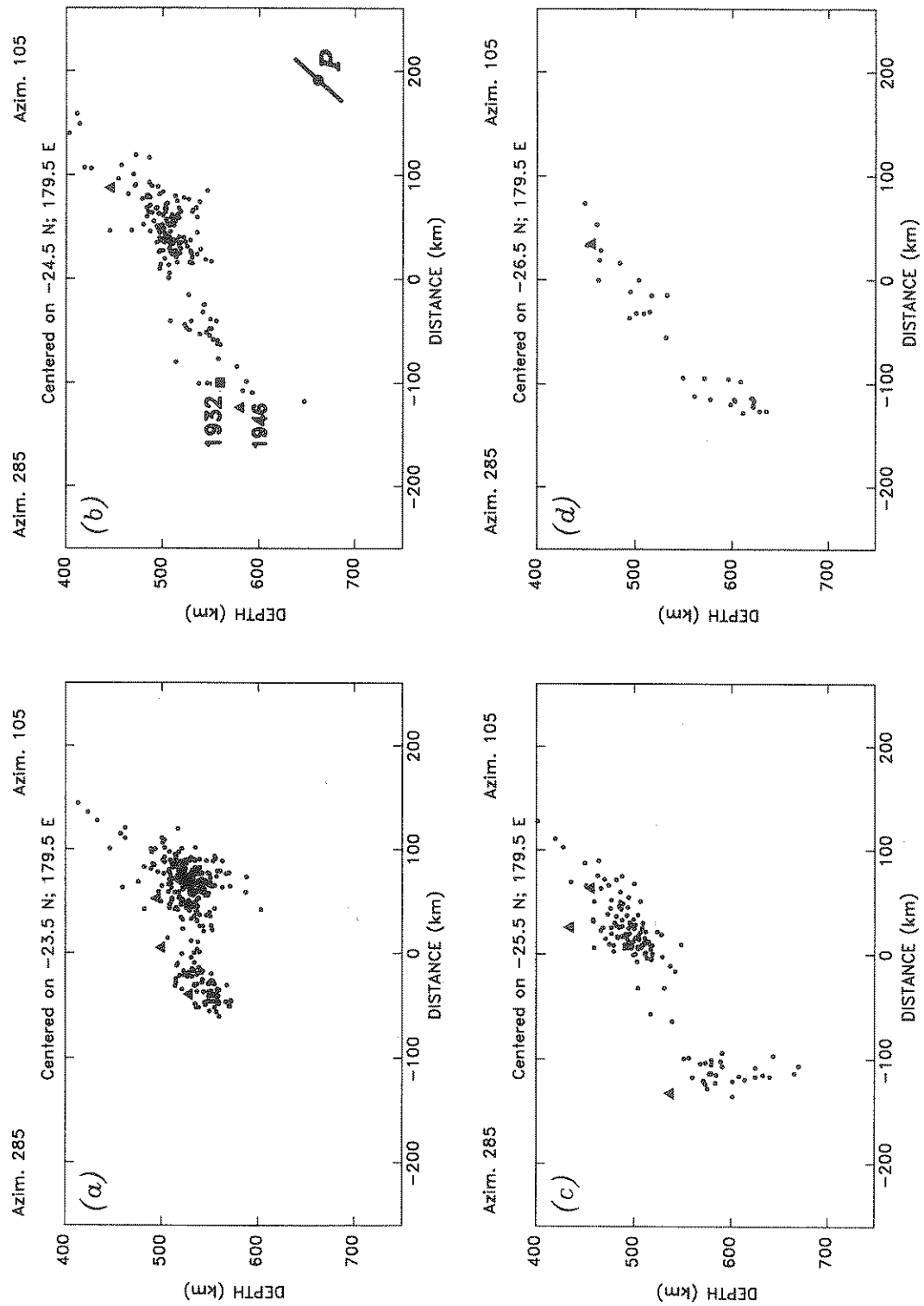Fig. 7 (continued). (b) Same as (a), looking northeast.

Fig. 8. Cross-sections of the Wadati–Benioff Zone in the vicinity of the 1932 hypocenter. Each figure represents a one-degree band of latitude: (a) 23°S to 24°S; (b) 24°S to 25°S; (c) 25°S to 26°S; (d) 26°S to 27°S. Note how the WBZ develops a claw-like extension to depths greater than 600 km, immediately to the south of the hypocentral zone. Dots represent 1964–1991 seismicity from Engdahl et al. (1997); square represents the 1932 deep shock; triangles indicate other large historical events (see Table 1). The symbol in the lower right corner of frame (b) shows the orientation of the P axis of the 1932 event.

which we write as $M_0 = 3.4(*/1.5) \times 10^{27}$ dyn cm. In this general context, the 1932 earthquake is most comparable to the 1994 Fiji earthquake, and remains definitely smaller (by a factor of 7 to 10 in M_0) than the gigantic Colombian and Bolivian shocks.

5. Discussion

While remaining well below those of the Bolivian and Colombian events, the moment measured for the 1932 deep Fiji earthquake is among the ten largest ever obtained for transition zone shocks; it is at least as big as the 1994 Fijian event, and thus could be the largest deep earthquake ever recorded in that subduction zone.

Fig. 7 shows three-dimensional views of the seismicity of the Tonga–Kermadec slab, using 1964–1991 hypocenters as relocated by Engdahl et al. (1997). The 1932 event is located in the Tonga slab, approximately 350 km from the major tear separating the latter from the more steeply dipping Kermadec segment. The hypocentral area is one of relatively complex geometry of the Wadati–Benioff Zone (W-BZ): immediately to the southwest of the hypocenter is a zone where seismicity extends deeper (to 670 km) than to the north (where it bottoms at 590 km). The 1932 event took place on the northern side of this feature, which appears claw-like in cross-section, and towards the front edge of the WBZ (Fig. 8). In addition, we relocated eight large historical earthquakes (with bulletin magnitudes $M \geq 6\frac{3}{4}$) whose original location was less than 250 km away from the 1932 main shock. Results are listed at the bottom of Table 1. Six of them relocate in the WBZ more than 120 km away from the 1932 event. The other two (26 Sep. and 08 Oct. 1946) relocate along the edges of the 'claw', only 73 and 31 km away, respectively. These results suggest that the three-dimensional picture of the WBZ would not be significantly changed by the inclusion of historical seismicity.

In this general framework, the 1932 event occurred in an area of regular seismic activity. This is in contrast with the largest deep South American shocks (1994, Bolivia; 1970, Colombia; 1921–1922, Peru) as well as with the 1954 Spanish earthquake, which all occurred in areas previously considered aseismic. Furthermore, the 1932 event took place both in a zone of significant distortion of the WBZ,

and towards the spatial extremity of the active seismogenic zone, in general agreement with the tentative observation of such trends for major transition zone earthquakes reported by Okal et al. (1996). Note that a similar situation applies to the 1994 Fiji event, located at the northern bend of the WBZ (Fig. 7), and to the 1994 Bolivian earthquake located in the large-scale jog of the South American slab (Kirby et al., 1995). It has been argued for a few years now that metastable phases such as olivine, whose presence is most probable inside the cold interior of subducting slabs, could give rise to seismicity in the transition zone through a rupture process known as transformational faulting accompanying the release of metastability (Kirby et al., 1996). In this general framework, stress concentrations near the spatial limits of metastability, or increased levels of stress in deformed portions of the slab could explain the preferential occurrence of large events in such environments.

The focal mechanism of the 1932 shock is characterized by down-dip compressional stress (50° dip towards N285°E). Although not comparable in size, a number of CMT solutions are available in the immediate vicinity of the hypocenter (Dziewonski et al., 1983, and subsequent quarterly updates; Huang et al., 1997). Fig. 4 shows that there is a wide scatter of geometries in the vicinity of the 1994 Fiji event, as also noted by Giardini and Lundgren (1995). However, the largest available CMT solution ($M_0 = 8.1 \times 10^{25}$ dyn cm on 15 February 1971 and only 34 km away from the 1932 hypocenter) has a mechanism virtually identical to the 1932 shock; both can be readily interpreted as releasing down-dip compressional stress.

6. Conclusions

(1) Our estimate of the moment of the 1932 deep Fiji earthquake ($3.4(*/1.5) \times 10^{27}$ dyn cm) makes it comparable to, but not significantly larger than, the 1994 Fiji deep shock. In this respect, it fits remarkably well the frequency–size population model of Okal and Kirby (1995), who advocated a return time of 64 years for events of this size in the Fiji–Tonga–Kermadec subduction zone. At any rate, the earthquake is definitely much smaller than the South American giants (Bolivia, 1970; Colombia, 1994).

(2) The focal mechanism obtained for the event featuring down-dip compression is readily interpreted as the probable release of the prevailing large-scale ambient stress. The mechanism is similar to that of the largest CMT solution available in the vicinity, a 1971 event which took place only 34 km away.

(3) The event is characterized both by source complexity (with three sub-events identifiable and relocated), and by the generation of five confirmed aftershocks over a period of less than a day. This supports the observation (Frohlich, 1989; Wiens et al., 1995) that Tonga–Fiji deep events have particularly sizable aftershock populations.

(4) The hypocentral area of the 1932 event shows significant background seismicity, but the earthquake took place on the edge of the active zone, and furthermore in an area of complex, deformed, geometry of the Wadati–Benioff Zone. Similar characteristics have often been observed for the very largest deep events, and may be related to the existence of enhanced stresses in or around fields of peridotite instability in the cold descending slabs.

Acknowledgements

References

Abe, K. and Kanamori, H., 1979. Temporal variation of the activity of intermediate and deep earthquakes. J. Geophys. Res., 84: 3589–3595.

Anonymous, 1932. Seismological Reports for April, May, June, 1932. Domin. Observ., Wellington, 20 pp.

Brunner, G.J., 1938. The deep earthquake of May 26, 1932 near the Kermadec Islands. Gerlands Beitr. Geophys., 53: 1–64.

Douglas, A., 1967. Joint hypocenter determination. Nature, 215: 47–48.

Dziewonski, A.M., Friedman, A., Giardini, D. and Woodhouse, J.H., 1983. Global seismicity of 1982: Centroid moment tensor solutions for 308 earthquakes. Phys. Earth Planet. Inter., 33: 76–90.

Engdahl, E.R., van der Hilst, R. and Buland, R.P., 1997. Global teleseismic earthquake relocation with improved travel times and procedures for depth relocation. Bull. Seismol. Soc. Am., in press.

Frohlich, C., 1989. The nature of deep-focus earthquakes. Annu. Rev. Earth Planet. Sci., 17: 227–254.

Giardini, D. and Lundgren, P.R., 1995. The June 9 Bolivia and March 9 Fiji deep earthquakes of 1994, II. Geodynamic implications. Geophys. Res. Lett., 22: 2281–2284.

Gutenberg, B., 1945. Magnitude determination for deep-focus earthquakes. Bull. Seismol. Soc. Am., 35: 117–130.

Gutenberg, B. and Richter, C.F., 1938. Depth and geographical distribution of deep-focus earthquakes. Geol. Soc. Am. Bull., 49: 249–288.

Gutenberg, B. and Richter, C.F., 1954. Seismicity of the Earth. Princeton Univ. Press, Princeton, NJ, 310 pp.

Huang, W.-C., Ekström, G., Okal, E.A. and Salganik, M.P., 1994. Application of the CMT algorithm to analog recordings of deep earthquakes. Phys. Earth Planet. Inter., 83: 283–297.

Huang, W.-C., Okal, E.A., Ekström, G. and Salganik, M.P., 1997. Centroid–Moment–Tensor solutions for deep earthquakes predating the digital era: The WWSSN dataset (1962–1976). Phys. Earth Planet. Inter., 99: 121–130.

International Seismological Summary, 1937. April, May, June. Oxford Univ., pp. 106–261.

Kanamori, H. and Cipar, J.J., 1974. Focal process of the great Chilean earthquake May 22, 1960. Phys. Earth Planet. Inter., 9: 128–136.

Kennett, B.L.N. and Engdahl, E.R., 1991. Travel times for global earthquake location and phase identification. Geophys. J. Int., 105: 429–465.

Kirby, S.H., Okal, E.A. and Engdahl, E.R., 1995. The 09 June 1994 great Bolivian deep earthquake: An exceptional deep earthquake in an extraordinary subduction zone. Geophys. Res. Lett., 22: 2233–2236.

Kirby, S.H., Stein, S., Okal, E.A. and Rubie, D., 1996. Deep earthquakes and metastable mantle phase transformations in subducting oceanic lithosphere. Rev. Geophys. Space Phys., 34: 261–306.

McComb, H.E. and West, C.J., 1931. List of seismological stations of the world. Bull. Natl. Res. Counc., 82, 119 pp.

Okal, E.A., 1979. Higher mode Rayleigh waves studied as an individual seismic phase. Earth Planet. Sci. Lett., 43: 162–167.

Okal, E.A., 1984. Intraplate seismicity of the southern part of the Pacific plate. J. Geophys. Res., 89: 10053–10071.

Okal, E.A., 1990. M_m: A mantle wave magnitude for intermediate and deep earthquakes. Pure Appl. Geophys., 134: 333–354.

Okal, E.A., 1992a. Use of the mantle magnitude M_m for the reassessment of the seismic moment of historical earthquakes, I. Shallow events. Pure Appl. Geophys., 139: 17–57.

Okal, E.A., 1992b. Use of the mantle magnitude M_m for the reassessment of the seismic moment of historical earthquakes, II. Intermediate and deep events. Pure Appl. Geophys., 139: 59–85.

Okal, E.A. and Jo, B.-G., 1983. Regional dispersion of first order overtone Rayleigh waves. Geophys. J. R. Astron. Soc., 72: 461–481.

Okal, E.A. and Kirby, S.H., 1995. Frequency–moment distribution of deep earthquakes: Implications for the seismogenic zone at the bottom of slabs. Phys. Earth Planet. Inter., 92: 169–187.

Okal, E.A., Kirby, S.H., Engdahl, E.R. and Huang, W.-C., 1996. Global distribution of large deep earthquakes and its possible significance. Eos, Trans. Am. Geophys. Union, 77(22): W140 (abstr.).

Russakoff, D., Ekström, G. and Tromp, J., 1996. A new analysis of the great 1970 Colombia deep earthquake and its isotropic component. Eos, Trans. Am. Geophys. Union, 77(46): F54 (abstr.).

Seismological Society of America 1980. Seismology Microfiche Publications from the Caltech Archives, Ser. II and III, edited by J.R. Goodstein, H. Kanamori and W.H.K. Lee. Berkeley, CA.

Stechschulte, V.C., 1932. The Japanese earthquake of March 29, 1928 and the problem of the depth of focus. Bull. Seismol. Soc. Am., 22: 81–137.

Stein, S. and Wiens, D.A., 1986. Depth determination for shallow teleseismic earthquakes: Methods and results. Rev. Geophys., 24: 806–832.

Stein, S., Okal, E.A. and Wiens, D.A., 1987. Application of modern techniques to analysis of historical earthquakes. In: W.H.K. Lee, H. Meyers and K. Shimazaki (Editors), Historical Seismograms and Earthquakes of the World. Academic Press, London, pp. 85–104.

Sverdrup, K.A. and Jordan, T.H., 1981. Teleseismic location techniques and their application to earthquake clusters in the Southcentral Pacific. Bull. Seismol. Soc. Am., 71: 1105–1130.

Wiens, D.A. and McGuire, J.J., 1995. The 1994 Bolivia and Tonga events: fundamentally different types of deep earthquakes? Geophys. Res. Lett., 22: 2245–2248.

Wiens, D.A., McGuire, J.J. and Shore, P.J., 1995. Systematic variations in deep earthquake aftershock production: different rates for different plates. Eos, Trans. Am. Geophys. Union, 76(46): F366 (abstr.).

Wysession, M.E., Okal, E.A. and Miller, K.L., 1991. Intraplate seismicity of the Pacific Basin, 1913–1988. Pure Appl. Geophys., 135: 261–359.